PERGAMON

International Journal of Heat and Mass Transfer 44 (2001) 1735–1749

International Journal of HEAT and MASS TRANSFER

www.elsevier.com/locate/ijhmt

Analysis of fluid flow and heat transfer interfacial conditions between a porous medium and a fluid layer

B. Alazmi, K. Vafai *

Department of Mechanical Engineering, The Ohio State University, 206 West 18th Avenue, Columbus, OH 43210-1107, USA

Received 21 April 2000; received in revised form 15 June 2000

Abstract

Different types of interfacial conditions between a porous medium and a fluid layer are analyzed in detail. Five primary categories of interface conditions were found in the literature for the fluid flow at the interface region. Likewise, four primary categories of interface conditions were found in the literature for the heat transfer at the interface region. These interface conditions can be classified into two main categories, slip and no-slip interface conditions. The effects of the pertinent parameters such as Darcy number, inertia parameter, Reynolds number, porosity and slip coefficients, on different types of interface conditions are analyzed while fluid flow and heat transfer in the neighborhood of an interface region are properly characterized. A systematic analysis of the variances among different boundary conditions establishes the convergence or divergence among competing models. It is shown that in general, the variances have a more pronounced effect on the velocity field and a substantially smaller effect on the temperature field and even a smaller effect on the Nusselt number distributions. For heat transfer interface conditions, all four categories generate results, which are quite close to each other for most practical applications. However, small discrepancies could appear for applications dealing with large values of Reynolds number and/or large values of Darcy number. Finally, a set of correlations is given for interchanging the interface velocity and temperature as well as the average Nusselt number among various models. © 2001 Elsevier Science Ltd. All rights reserved.

1. Introduction

Fluid flow and heat transfer characteristics at the interface region in systems which consist of a fluid-saturated porous medium and an adjacent horizontal fluid layer have received considerable attention. This attention stems from the wide range of engineering applications such as electronic cooling, transpiration cooling, drying processes, thermal insulation, porous bearing, solar collectors, heat pipes, nuclear reactors, crude oil extraction and geothermal engineering. The work of Beavers and Joseph [1] was one of the first attempts to study the fluid flow boundary conditions at the interface region. They performed experiments and detected a slip in the velocity at the interface. Neale and Nader [2] presented one of the earlier attempts regarding this type of boundary condition in porous medium. In this study, the authors proposed a continuity in both the velocity and the velocity gradient at the interface by introducing the Brinkman term in the momentum equation for the porous side. Vafai and Kim [3] presented an exact solution for the fluid flow at the interface between a porous medium and a fluid layer including the inertia and boundary effects. In this study, the shear stress in the fluid and the porous medium were taken to be equal at the interface region. Vafai and Thiyagaraja [4] analytically studied the fluid flow and heat transfer for three types of interfaces, namely, the interface between two different porous media, the interface separating a porous medium from a fluid region and the interface between a porous medium and an impermeable medium. Continuity of shear stress and heat flux were taken into account in their study while employing the Forchheimer-Extended Darcy equation in their analysis. Other studies consider the same set of

* Corresponding author. Tel.: +1-614-292-6560; fax: +1-614-292-3163.

E-mail address: vafai.1@osu.edu (K. Vafai).

0017-9310/01/$ - see front matter © 2001 Elsevier Science Ltd. All rights reserved.
PII: S0017-9310(00)00217-9

Nomenclature

c_p	specific heat at constant pressure (J kg^{-1} K^{-1})
Da	Darcy number, K/H^2
F	geometric function defined in Eq. (4)
h	heat transfer coefficient (W m^{-2} K^{-1})
H	height of the fluid layer (m)
k	thermal conductivity (W m^{-1} K^{-1})
K	permeability (m^2)
Nu	local Nusselt number
$\overline{Nu}$	average Nusselt number
P	pressure (N/m^2)
Re	Reynolds number, $u_\infty H/\nu_f$
T	temperature (K)
T_m	mean temperature (K)
u	velocity in x-direction (m s^{-1})
u_{int}	interface velocity (m s^{-1})
U	non-dimensional velocity, u/u_∞
U_{int}	non-dimensional interface velocity
x, y	Cartesian coordinates (m)
X, Y	non-dimensional coordinates, x/H and y/H

Greek symbols

α	thermal diffusivity (m^2 s^{-1})
α^*	velocity slip coefficient in Table 1
α_T	temperature slip coefficient in Table 2
ε	porosity
ϕ	parameter in Table 2
Λ	inertia parameter, $\varepsilon FH/K^{1/2}$
μ	kinematics viscosity (kg m^{-1} s^{-1})
ν	dynamic viscosity (m^2 s^{-1})
ρ	density (kg m^{-3})
Θ	dimensionless temperature, $(T_w - T)/(T_w - T_\infty)$

Subscripts

eff	effective property
f	fluid
int	interfacial
w	wall
∞	free stream
−	plain medium side
+	porous medium side

boundary conditions for the fluid flow and heat transfer used in [4] such as [5–8].

Ochoa-Tapia and Whitaker [9,10] have proposed a hybrid interface condition (a hybrid between models 2 and 5 discussed later on) in which a jump in the shear stress at the interface region is assumed. In their study, the shear stress jump is inversely proportional to the permeability of the porous medium. This proposed set of interface conditions was used in [11–15]. More recently, Ochoa-Tapia and Whitaker [16] have presented another shear stress jump boundary condition where the inertia effects become important. The same investigators [17] have also presented another hybrid interface condition for the heat transfer part in which they introduce a jump condition to account for a possible excess in the heat flux at the interface. Sahraoui and Kaviany [18] have proposed yet another hybrid interface condition for the heat transfer part. They used the continuity of the heat flux at the interface along with a slip in the temperature at the interface. The main focus of the present study is to critically examine the differences in the fluid flow and heat transfer characteristics due to different interface conditions, including all the aforementioned models. The current study complements a prior work by Alazmi

Table 1
Primary categories of fluid flow interface conditions between a porous medium and a fluid layer

Model	Velocity	Velocity gradient	Refs.
1	$u_+ = u_-$	$\left.\frac{du}{dy}\right\|_+ = \left.\frac{du}{dy}\right\|_-$	[2,3,5,23]
2	$u_+ = u_-$	$\mu_{eff}\left.\frac{du}{dy}\right\|_+ = \mu\left.\frac{du}{dy}\right\|_-$	[4,6,7]
3	$u_+ = u_-$	$\frac{\mu}{\varepsilon}\left.\frac{du}{dy}\right\|_+ - \mu\left.\frac{du}{dy}\right\|_- = \beta_1\frac{\mu}{\sqrt{K}}u$	[9–15]
4	$u_+ = u_-$	$\frac{\mu}{\varepsilon}\left.\frac{du}{dy}\right\|_+ - \mu\left.\frac{du}{dy}\right\|_- = \beta_1\frac{\mu}{\sqrt{K}}u + \beta_2\rho u^2$	[16]
5[a]		$\left.\frac{du}{dy}\right\|_- = \frac{\alpha^*}{\sqrt{K}}(u_{int} - u_\infty)$	[1,21]

[a] A Forchheimer term is added to the momentum equation in the porous side for the purpose of comparison.

Table 2
Primary categories of heat transfer interface conditions between a porous medium and a fluid layer

Model	Temperature	Temperature gradient	Refs.
I	$T_+ = T_-$	$k_{\text{eff}}\frac{\partial T_-}{\partial y} = k_{\text{f}}\frac{\partial T_+}{\partial y}$	[2,4–8,13–15,23]
II	$T_+ = T_-$	$\phi + k_{\text{f}}\frac{\partial T}{\partial y}\Big\|_- = k_{\text{eff}}\frac{\partial T}{\partial y}\Big\|_+$	[17]
III	$\frac{\mathrm{d}T}{\mathrm{d}y}\Big\|_+ = \frac{\alpha_{\text{T}}}{\lambda}(T_+ - T_-)$	$k_{\text{eff}}\frac{\partial T_-}{\partial y} = k_{\text{f}}\frac{\partial T_+}{\partial y}$	[18], using fluid flow of model 1
IV	$\frac{\mathrm{d}T}{\mathrm{d}y}\Big\|_+ = \frac{\alpha_{\text{T}}}{\lambda}(T_+ - T_-)$	$k_{\text{eff}}\frac{\partial T_-}{\partial y} = k_{\text{f}}\frac{\partial T_+}{\partial y}$	[18], using fluid flow of model 3

and Vafai [19] in which they presented a comprehensive analysis of variants within the transport models in porous media. In their study, four major categories namely, constant porosity, variable porosity, thermal dispersion and local thermal non-equilibrium were considered in great detail.

2. Analysis

A comprehensive synthesis of literature revealed five primary categories for interface conditions for the fluid flow and four primary forms of interface conditions for the heat transfer between a porous medium and a fluid layer. Table 1 summarizes the models for the fluid flow part while Table 2 summarizes the models for the heat transfer part. The fundamental configuration used by Vafai and Kim [3], representing the interface region between a porous medium and a fluid layer, is used in the current study. This configuration consists of a fluid layer sandwiched between a porous medium from above and a solid boundary from below. The physical configuration and the coordinate system are shown in Fig. 1 (a). For the porous region, the governing equations are [20]:

$$\frac{\rho_{\text{f}}}{\varepsilon}\langle(V\cdot\nabla)V\rangle = -\frac{\mu}{K}\langle V\rangle - \frac{\rho_{\text{f}}F\varepsilon}{\sqrt{K}}[\langle V\rangle\cdot\langle V\rangle]J + \frac{\mu}{\varepsilon}\nabla^2\langle V\rangle - \nabla\langle P\rangle, \tag{1}$$

$$\langle V\rangle\cdot\nabla\langle T\rangle = \frac{\alpha_{\text{eff}}}{\varepsilon}\nabla^2\langle T\rangle, \tag{2}$$

where

$$\alpha_{\text{eff}} = \frac{k_{\text{eff}}}{\rho_{\text{f}}c_{\text{pf}}}, \tag{3a}$$

$$k_{\text{eff}} = \varepsilon k_{\text{f}} + (1-\varepsilon)k_{\text{s}}. \tag{3b}$$

The governing equations for the fluid region can be written as [3,4]:

$$\mu\nabla^2\langle V\rangle = \nabla\langle P\rangle, \tag{4}$$

$$\langle V\rangle\cdot\nabla\langle T\rangle = \alpha_{\text{f}}\nabla^2\langle T\rangle, \tag{5}$$

where

$$\alpha_{\text{f}} = \frac{k_{\text{f}}}{\rho_{\text{f}}c_{\text{pf}}}. \tag{6}$$

The pertinent dimensionless parameters for this problem are [3]:

$$Da = \frac{K}{H^2}, \tag{7a}$$

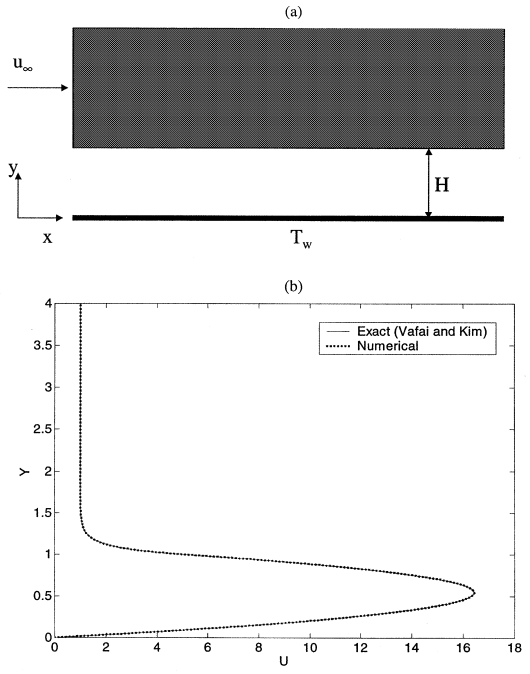

Fig. 1. (a) Schematic of the physical model and the coordinate system. (b) Comparison between the exact solution of Vafai and Kim and the present numerical results.

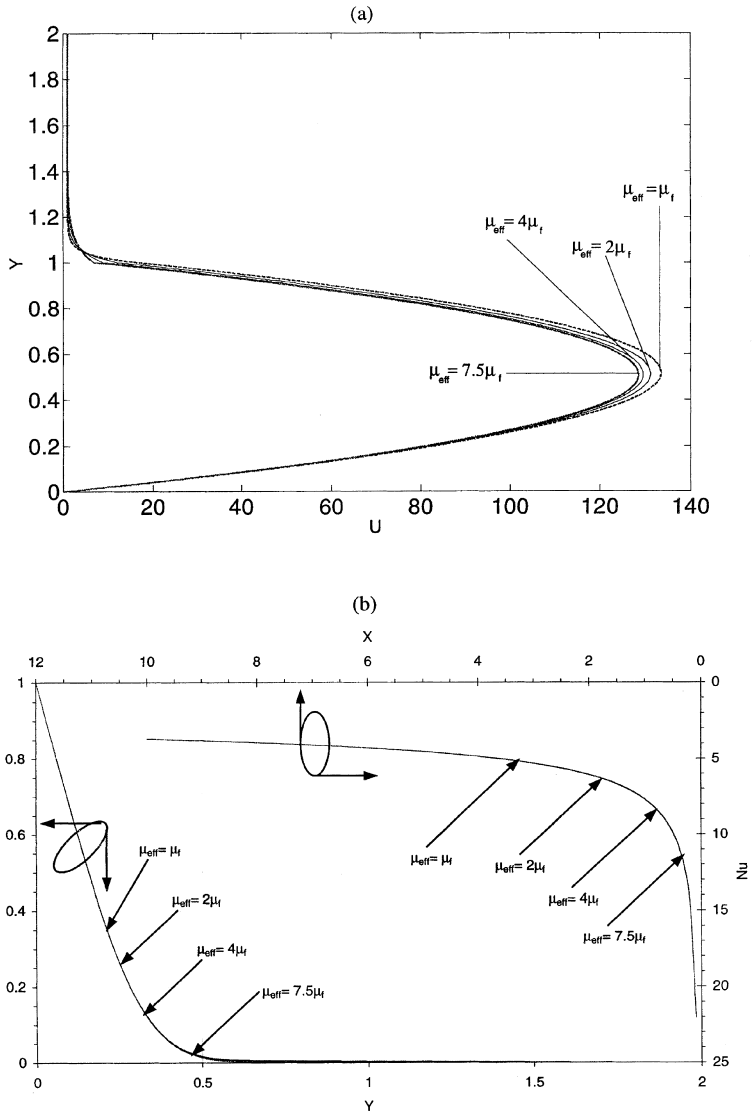

Fig. 2. Effect of changing the effective viscosity on: (a) velocity field; (b) temperature field and Nusselt number distribution for the interface between a porous medium and a fluid layer, $\varepsilon = 0.7,\ \Lambda = 1.0,\ Da = 10^{-3},\ Re = 1.0$.

$$Re = \frac{u_\infty H}{\nu_f}, \tag{7b}$$

$$\Lambda = \frac{F\varepsilon H}{\sqrt{K}}. \tag{7c}$$

Primary categories of interface conditions utilized in the literature for the fluid flow are given in Table 1, while those for the heat transfer are given in Table 2.

3. Results and discussion

A comprehensive analysis of fluid flow and heat transfer for the interface region between a fluid layer and an adjacent porous layer can be found in [4]. Therefore, the current study concentrates on analyzing and synthesizing the effects of different interface conditions. The presentation of the results in the current study is given in terms of the velocity fields for models given in Table 1 and in terms of temperature and Nusselt number distributions for models given in Table 2. In presenting the results it is useful to introduce the following dimensionless variables [3]:

$$X = \frac{x}{L}, \quad Y = \frac{y}{H},$$

$$U = \frac{u}{u_\infty}, \quad \Theta = \frac{(T - T_w)}{(T - T_\infty)} \tag{8}$$

The local Nusselt number for the lower wall is defined as:

$$Nu = \frac{hH}{k_f}, \tag{9}$$

where h_x is the local heat transfer coefficient at the wall, which is defined as

$$h = \frac{H}{(T_w - T_m)} \left.\frac{\partial T}{\partial y}\right|_{y=0}. \tag{10}$$

3.1. Fluid flow

Comparison between the present numerical results and the exact solution of Vafai and Kim [3] is shown in Fig. 1(b). Considering the first two models in Table 1, it can be seen that model 1 becomes identical to model 2 when the effective viscosity of the porous medium equals the viscosity of the fluid. For model 2, when there is a significant difference between the viscosity of the fluid and the effective viscosity of the porous medium, the slope of the velocity profile in the porous medium is not the same as the slope on the other side of the interface. On the other hand, the velocity gradients for model 1 are equal on both sides. It should be noted that in the current study, based on the analysis presented in [20], the effective viscosity of the porous medium for model 2 is taken to be μ_f/ε. Therefore, for a higher porosity medium, the value of the effective viscosity is close to that of the fluid's. Models 3 and 4 present a jump in the shear

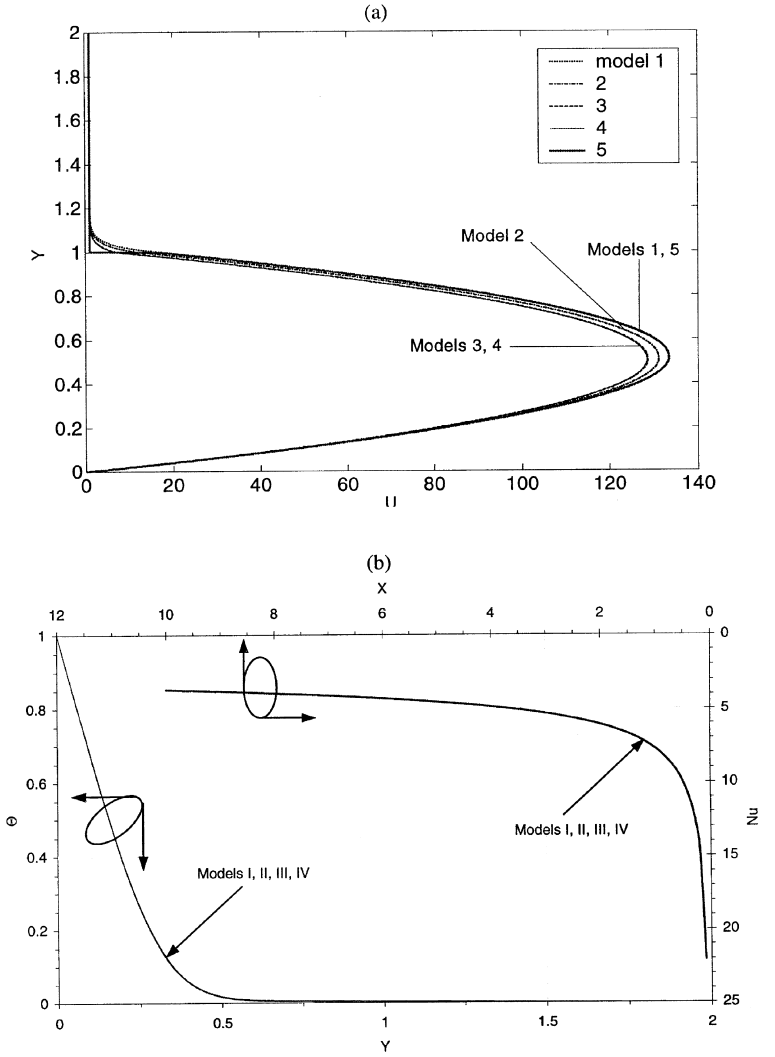

Fig. 3. (a) Velocity field; (b) temperature field and Nusselt number distribution for the interface between a porous medium and a fluid layer, $\varepsilon = 0.7$, $\Lambda = 1.0$, $Da = 10^{-3}$, $Re = 1.0$, $\beta_1 = 1.0$, $\beta_2 = 1.0$, $\alpha_T = 10.0$, $\phi = 10$.

stress while model 5 introduces a slip in the velocity at the interface region.

When the inertia effects are negligible, model 4 becomes identical to model 3. Therefore, model 3 is a special case of model 4. Neale and Nader [2] proposed a mathematical representation for the slip coefficient for model 5, they predicted that $\alpha^* = \sqrt{(\mu_{\text{eff}}/\mu)}$. Model 5 indicates that the velocity gradient in the fluid side is proportional to the difference between the interfacial velocity and the free stream velocity in the porous medium while inversely proportional to the permeability of the porous medium. The velocity slip coefficient α^* for model 5 is determined numerically by matching the velocity gradient of model 5 for each individual case according to the physical parameters for this case [21]. According to the experimental study of Gilver and Altobelli [22], the ratio of the effective viscosity, μ_{eff}, to the fluid viscosity, μ_{f}, is in the range of $5.1 < \mu_{\text{eff}}/\mu_{\text{f}} < 10.9$. A mean value of 7.5 was recommended by this study. Physically this range of values appears to be quite high. Nevertheless, a side study for the effect of choosing the effective viscosity is performed in this study and

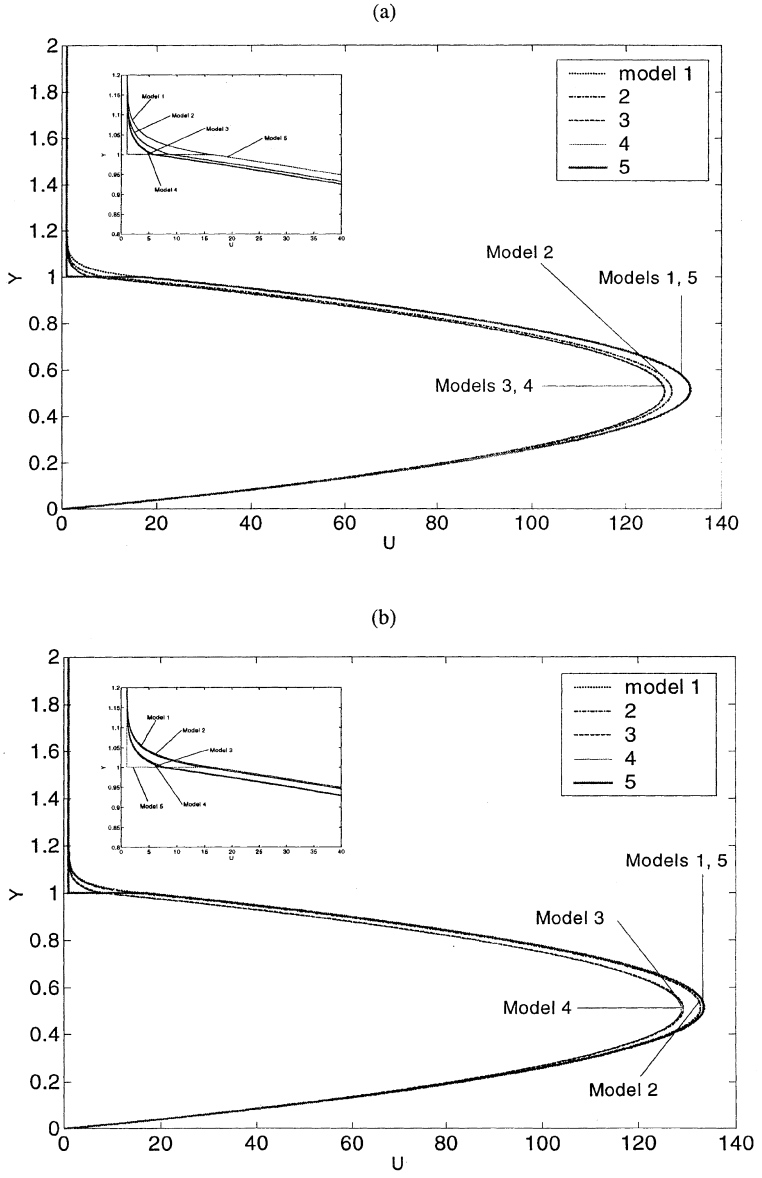

Fig. 4. Effect of porosity variation on the velocity field for the interface between a porous medium and a fluid layer, $\Lambda = 1.0$, $Da = 10^{-3}$, $Re = 1.0$, $\beta_1 = 1.0$, $\beta_2 = 1.0$. (a) $\varepsilon = 0.5$, (b) $\varepsilon = 0.9$.

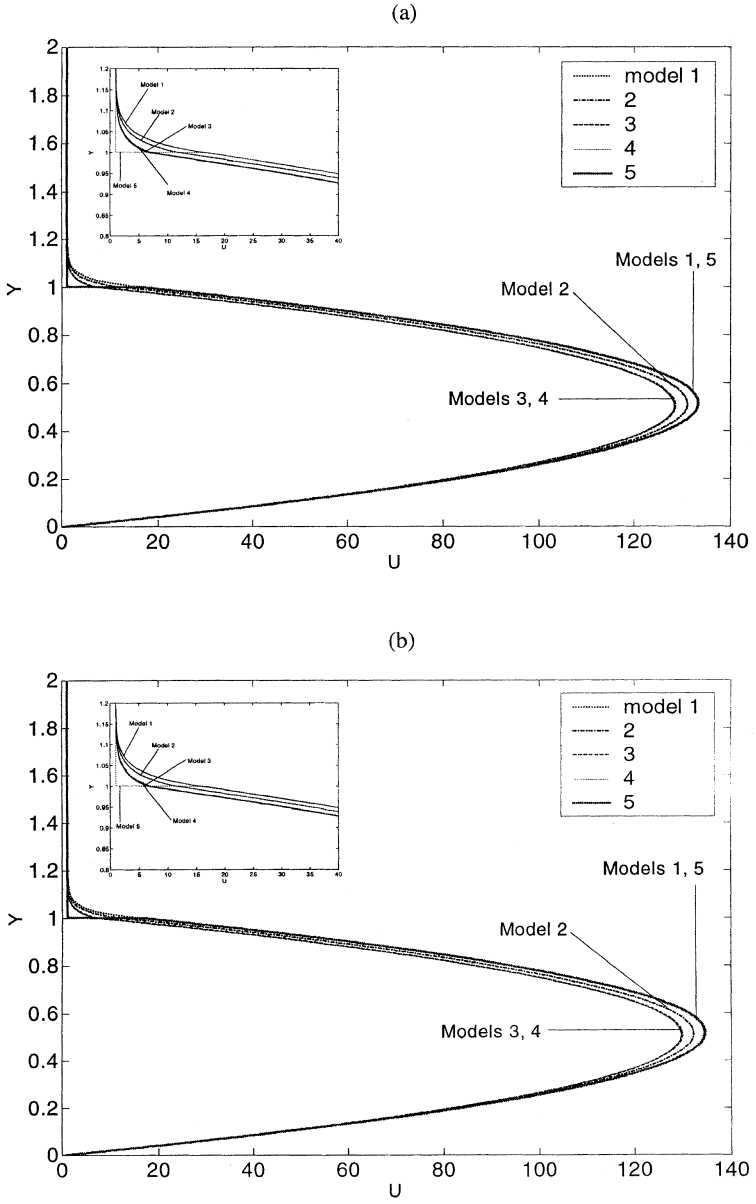

Fig. 5. Effect of inertia parameter variation on the velocity field for the interface between a porous medium and a fluid layer, $\varepsilon = 0.7$, $Da = 10^{-3}$, $Re = 1.0$, $\beta_1 = 1.0$, $\beta_2 = 1.0$. (a) $\Lambda = 0.1$, (b) $\Lambda = 10.0$.

presented in Fig. 2. Fig. 2(a) shows that changing the effective viscosity from μ_f to $7.5\mu_f$ has a relatively minor effect on the velocity profiles considering such a wide range of variations for the effective viscosity. The smaller velocity peak and interfacial velocity are associated with the highest effective viscosity. The effect of changing the effective viscosity on the temperature and Nusselt number distributions is shown in Fig. 2(b). It is clear that changing the effective viscosity even within such a wide range has an insignificant effect on the thermal field.

The comparative representation of velocity, temperature and Nusselt number given in Fig. 3 will be used as a baseline for studying the effects of different pertinent parameters. Comparisons between the five primary fluid interface conditions are given in Figs. 4–9. Fig. 3(a) is used as a baseline in which moderate values of the pertinent parameters are used. Fig. 4 shows the effect of porosity variation on the velocity field. It is clear that models 1 and 5 are unaffected by changing the porosity, this is expected as the boundary conditions in these models do not include a porosity term. Model 2 is the

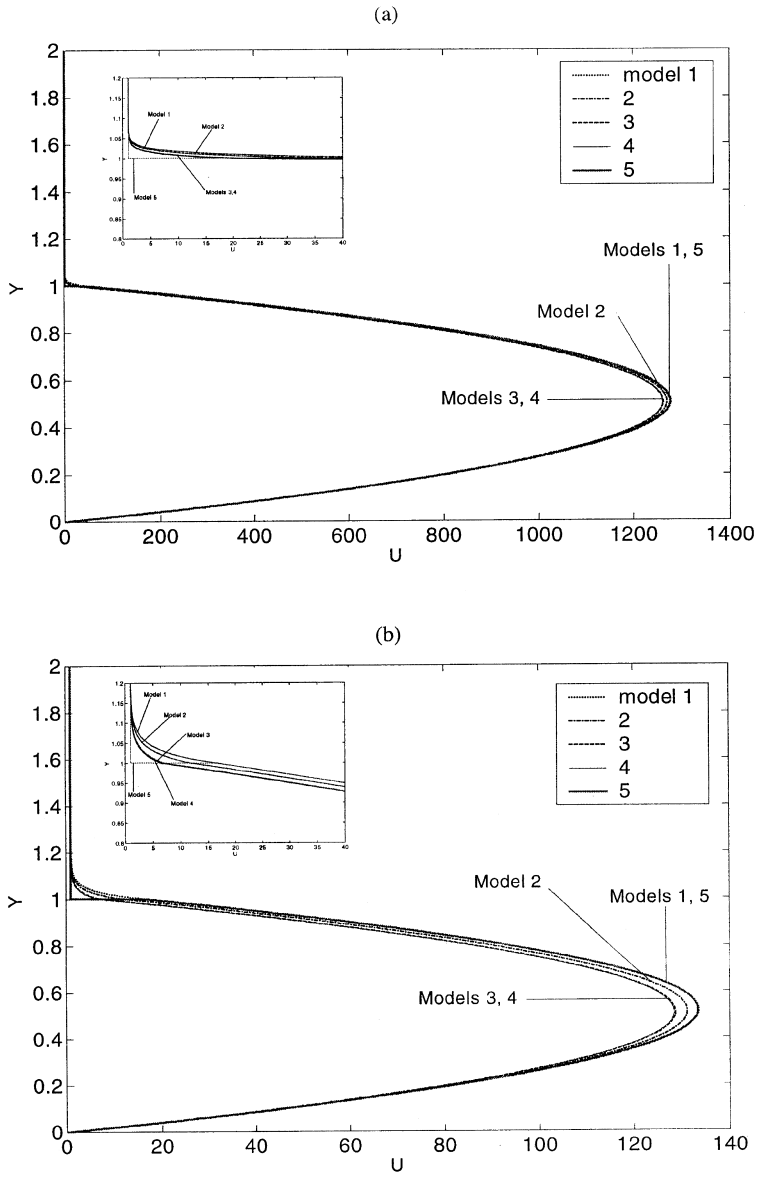

Fig. 6. Effect of Darcy number variation on the velocity field for the interface between a porous medium and a fluid layer, $\varepsilon = 0.7,\ \Lambda = 1.0,\ Re = 1.0,\ \beta_1 = 1.0,\ \beta_2 = 1.0$. (a) $Da = 10^{-4}$, (b) $Da = 10^{-3}$.

most affected by changing the porosity. An increase in the porosity causes model 2 to approach models 1 and 5 and a decrease in the porosity drives it in the opposite direction, i.e., toward models 3 and 4. In other words, higher porosity creates a higher peak velocity and smaller porosity creates a smaller peak velocity for model 2 in the plain medium.

The effect of variations in the inertia parameter is shown in Fig. 5. It is clear that an increase in the inertia parameter results in a slightly larger peak velocity for model 5 as compared to model 1. At the same time, an increase in the inertia parameter results in a smaller interfacial velocity for the first four models and a slightly larger interfacial velocity for the fifth model. The slight increase in the interfacial velocity for model 5 may be ascribed to the fact that this is the only model that does not account for the boundary effect in the momentum equation within the porous medium. The effect of Darcy number variation on the velocity field is shown in Fig. 6. It can be seen that for smaller Darcy numbers, the velocity profiles of all the five primary models are very close to each other, while large Darcy numbers induces a discrepancy among the models. This is because higher Darcy numbers translate into higher permeabilities in the porous side of

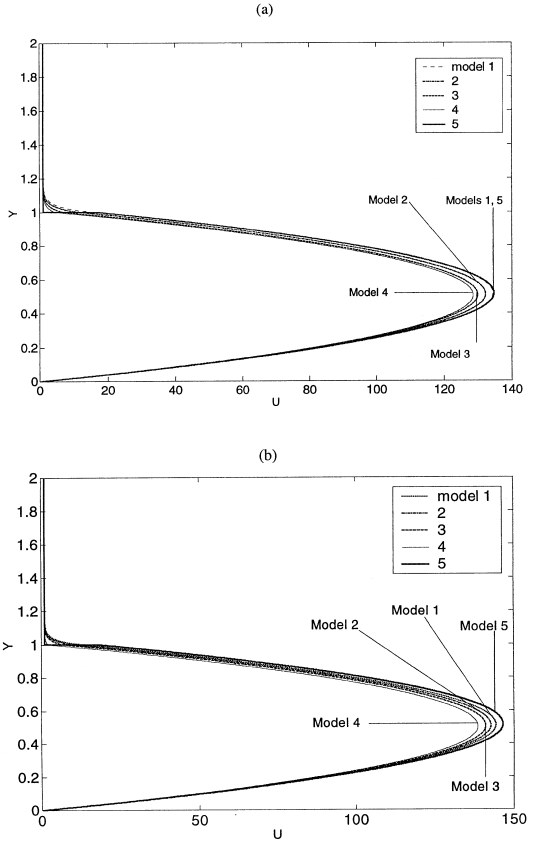

Fig. 7. Effect of Reynolds number variation on the velocity field for the interface between a porous medium and a fluid layer, $\varepsilon = 0.7,\ \Lambda = 10.0,\ Da = 10^{-3},\ \beta_1 = 1.0,\ \beta_2 = 1.0$. (a) $Re = 10.0$, (b) $Re = 100.0$.

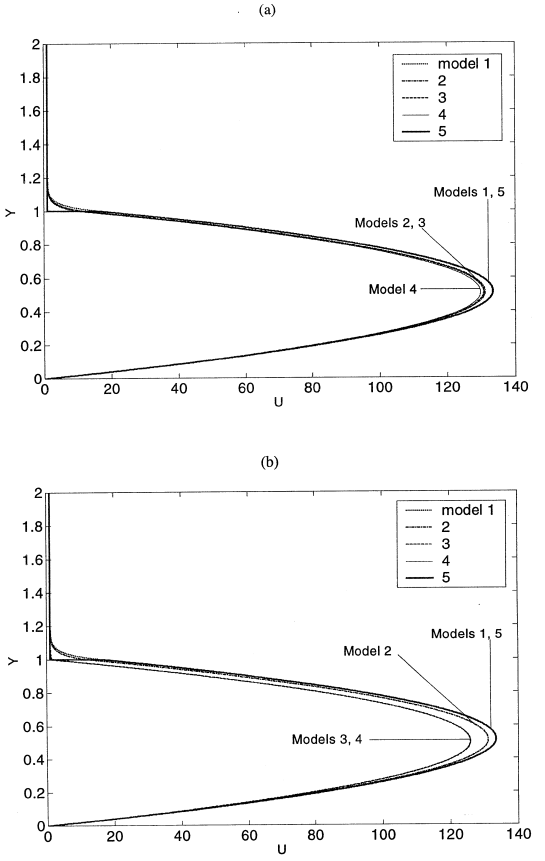

Fig. 8. Effect of β_1 variation on the velocity field for the interface between a porous medium and a fluid layer, $\varepsilon = 0.7,\ \Lambda = 1.0,\ Da = 10^{-3},\ Re = 1.0,\ \beta_2 = 1.0$. (a) $\beta_1 = 0.1$, (b) $\beta_1 = 10.0$.

the interface, which in turn results in a smaller ratio between the average velocity in the plain medium and the Darcian velocity. As a result of this smaller velocity ratio, the discrepancy between these models becomes more pronounced. However, it should be noted that for most practical applications $Da > 10^{-4}$ and as such the variation among the five models becomes less significant.

The effect of variations in Reynolds number is shown in Fig. 7. For larger Reynolds numbers the deviation between the velocity profiles for models 3 and 4 increases due to the presence of u^2 term in the interface condition for model 4. Reynolds number has a similar effect as the inertia parameter had on models 1 and 5. A similar result was found in [3]. Fig. 8 shows the effect of variations in the coefficient β_1. It indicates that for smaller values of β_1 the velocity profiles for models 2 and 3 collapse on each other. On the other hand, for larger β_1, velocity profiles for models 3 and 4 approach each other. This is because the linear term in the interface condition for model 4 becomes more dominant for larger values of β_1.

Large values of β_1 may cause a sharp change in the velocity gradient on both sides of the interface as shown in Fig. 8(b). The effect of variations in parameter β_2 on the velocity field is shown in Fig. 9. Smaller values of β_2 causes the velocity profile for model 4 to collapse on that for model 3 while larger values of β_2 increases the divergence between these two models and creates a sharper slope for the velocity profile for model 4.

In general, models 1 and 5 are closer to each other while models 3 and 4 are closer to each other. Model 2 usually falls in between the results for models 1, 5 and models 3, 4. Interfacial velocities for models 2–5 in terms of the interfacial velocity for model 1 and pertinent parameters such as the Darcy number, the Reynolds number, the inertia parameter and the porosity are given below:

$$U_{\mathrm{int}2} = \Big[-0.057 + 1.0194\varepsilon^{0.8762} + 0.00082544\Lambda + 0.0363(1000Da)^{0.3893} + 0.0010228Re \Big] U_{\mathrm{int}1}, \tag{11}$$

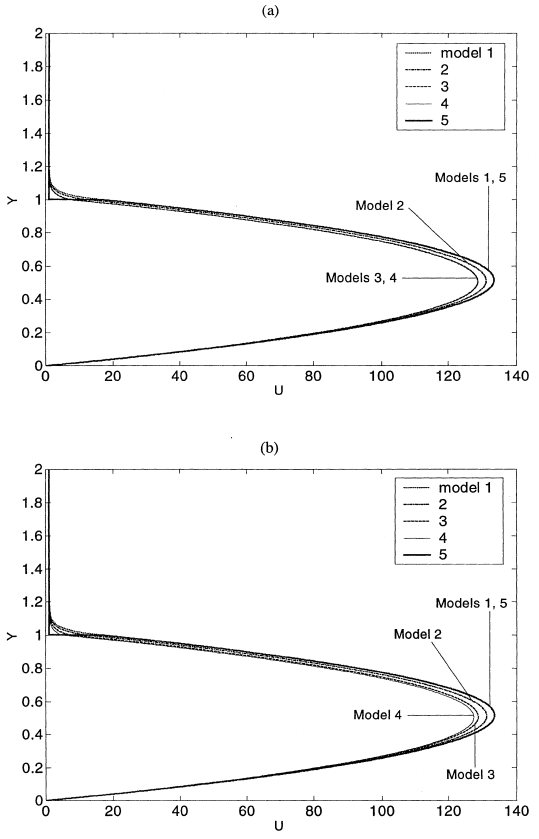

Fig. 9. Effect of β_2 variation on the velocity field for the interface between a porous medium and a fluid layer, $\varepsilon = 0.7$, $\Lambda = 1.0$, $Da = 10^{-3}$, $Re = 1.0$, $\beta_1 = 1.0$. (a) $\beta_2 = 0.1$, (b) $\beta_2 = 10.0$.

$$U_{\text{int3}} = \left[0.7077\varepsilon + 0.0202\Lambda - 54.9355Da^{11.7265} - 0.0082205Re - 0.053\beta_1\right] U_{\text{int1}}, \tag{12}$$

$$U_{\text{int4}} = [-14.9258 + 0.4185\varepsilon + 0.0012816\Lambda + 15.1505(1000Da)^{0.000643} - 0.0117Re - 0.0848\beta_1 + 0.0050702\beta_1^2 - 0.0129\beta_2] U_{\text{int1}}, \tag{13}$$

$$U_{\text{int5}} = [1.0107 - 0.169\varepsilon + 0.0077721\Lambda + 58.9397Da + 0.005532Re] U_{\text{int1}}. \tag{14}$$

In the above correlations, U_{int1} refers to the interface velocity based on model 1 and U_{int2}, U_{int3}, U_{int4} and U_{int5} refer to interface velocities based on models 2, 3, 4 and 5, respectively.

3.2. Heat transfer

Fig. 2(b) shows the temperature profiles and the local Nusselt number distributions for different ratios of $\mu_{\text{eff}}/\mu_{\text{f}}$. In this figure, the temperature and Nusselt number distributions for the entire wide range of variations in $\mu_{\text{eff}}/\mu_{\text{f}}$ are quite close to each other. The first type of heat transfer interface condition, model I is based on a continuity of temperature as well as heat flux at the interface region. The second model includes a jump in the heat flux at the interface region. As a logical extension the fluid flow model 1 is in conjunction with the heat transfer models I and II. The third (III) and the fourth (IV) heat transfer interface condition models have a jump in the temperature at the interface. However, the heat transfer interface model III utilizes the fluid flow model 1 while thermal model IV utilizes the fluid flow model 3.

The effects of the pertinent parameters on the temperature and Nusselt number distributions are shown in Figs. 10–13. Fig. 3(b) is used as the datum for temperature and Nusselt number comparisons. Fig. 10(a) shows the effect of porosity. Higher porosity results in a better agreement between models I and II while it decreases the discrepancies between the interfacial temperatures for models III and IV. In other words, higher porosity causes the results for fluid flow models 1 and 3 to be closer to each other, which in return coalesces the results for models III and IV.

The effects of inertia parameter variation are shown in Fig. 10(b). It has a relatively insignificant effect on the convergence or divergence of the temperature and Nusselt number profiles for the four models shown in Table 2. However, a careful examination indicates an increase in the inertia parameter produces convergence in the interfacial temperature for all the four models. This is due to the higher values of the inertia parameter, which results in larger convective heat transfer, which in turn decreases the effect of different interface conditions on the heat transfer results.

The effects of Darcy number variation, *Da*, are shown in Fig. 11(a). It is clear that for more practical values of Darcy number, all the four models displayed in Table 2 converge. For very large Darcy numbers, the discrepancy in the interfacial temperatures for the four models becomes more pronounced. Model IV has the highest interface temperature, model III has the next highest while models I and II have the lowest interfacial temperatures. However, the Nusselt numbers for the first three models are very close to each other with a slight deviation from the fourth model as seen in Fig. 11(a). Fig. 11(b) displays the effect of Reynolds number variation on the temperature field and the Nusselt number amongst the four models. As the Reynolds number increases a better agreement is achieved among the four models.

The effect of variations in β_1 is shown in Fig. 12(a). It is found that higher values of β_1 create a slightly higher interfacial temperature for model IV while smaller values of β_1 result in a closer agreement among the other

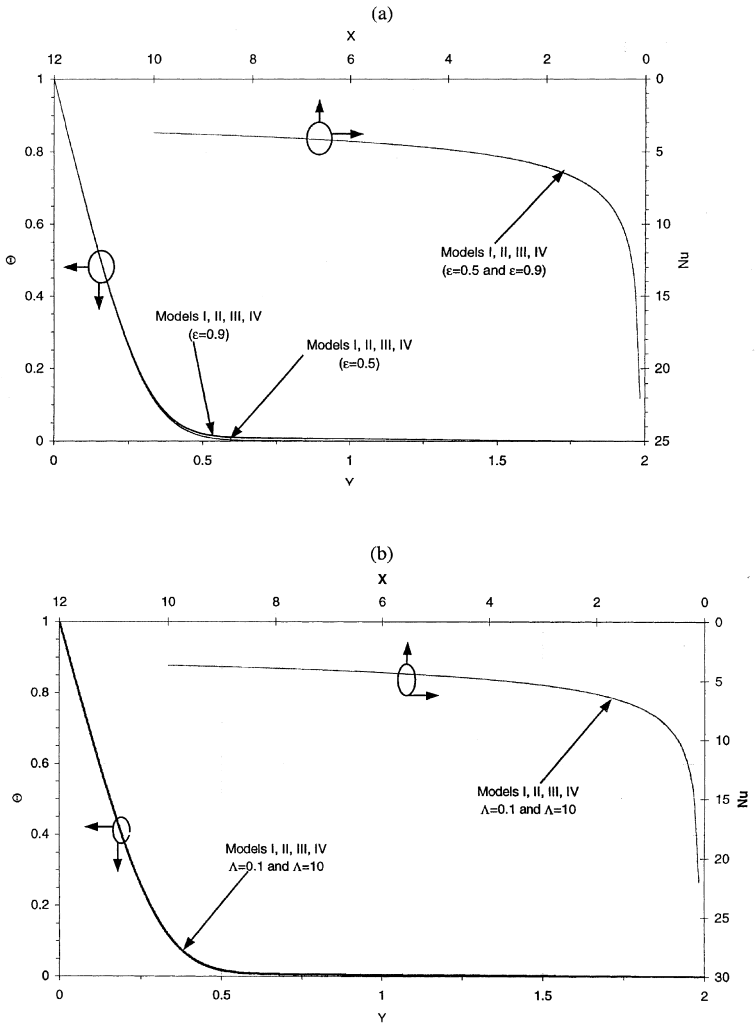

Fig. 10. Temperature field and Nusselt number distribution for the interface between a porous medium and a fluid layer, $Da = 10^{-3}$, $Re = 1.0$, $\beta_1 = 1.0$, $\alpha_T = 10.0$, $\phi = 10.0$. (a) Effect of porosity variation, $\Lambda = 1.0$, (b) effect of inertial parameter variation, $\varepsilon = 0.7$.

three models. However, overall all four models are in very close agreement even for significant variations in β_1. Fig. 12(b) shows the effect of variations in the temperature slip coefficient on temperature and Nusselt number profiles. It can be seen that the effect of the temperature slip coefficient is insignificant compared to the effects of the Darcy number and the Reynolds number. Finally, the effect of variations in ϕ is shown in Fig. 13. As can be seen for larger ϕ, the temperature distribution for model II in the non-porous region starts to deviates from the other three models. However, the effect of parameter ϕ on the Nusselt number is insignificant. This is because the temperature gradient at the lower surface is not significantly affected by changing ϕ. In general, for most cases the results obtained from all the four models are quite close to each other. However, for few cases described earlier, there are some minor deviations. However, even those deviations still can be considered insignificant. Interfacial temperatures for models II, III and IV in terms of the pertinent parameters and the non-dimensional interfacial temperature of the first model are given below:

$$\Theta_{\text{int2}} = [1.0132 - 0.0077072\varepsilon - 0.0010277\Lambda + 1.0272Da - 0.0063711Re - 0.0024633\phi]\Theta_{\text{int1}}, \quad (15)$$

$$\Theta_{\text{int3}} = [0.3765 + 0.6459\varepsilon - 0.0194\Lambda + 48.2034Da - 0.0444Re - 0.0023708\alpha_T]\Theta_{\text{int1}}, \quad (16)$$

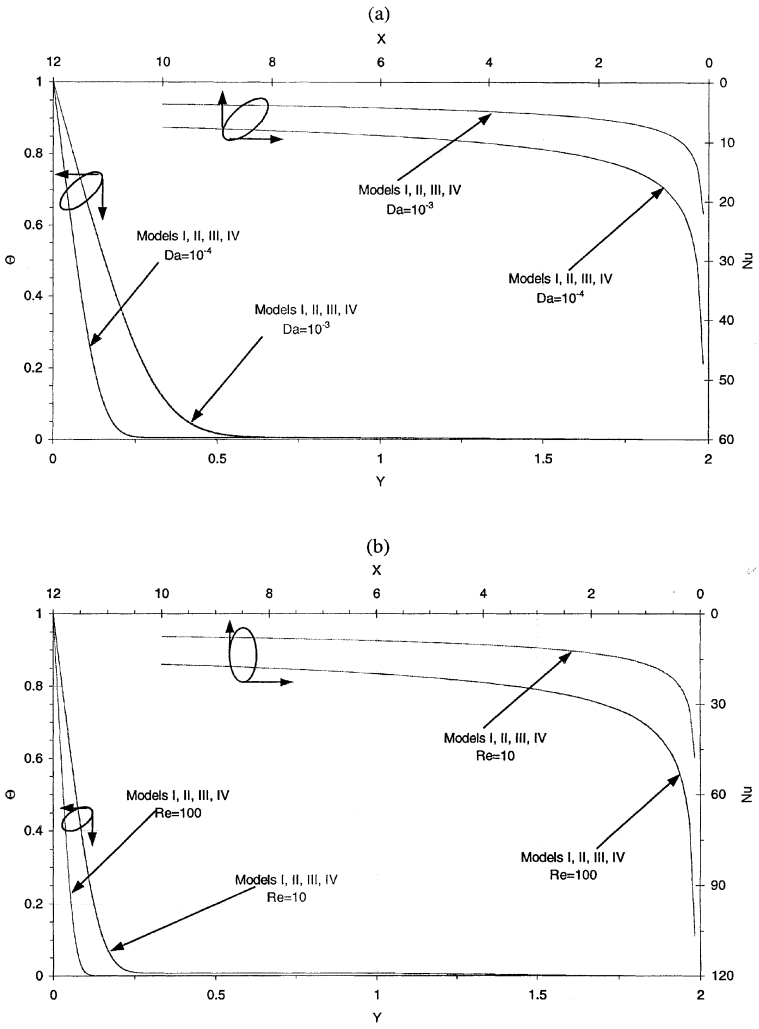

Fig. 11. Temperature field and Nusselt number distribution for the interface between a porous medium and a fluid layer, $\varepsilon = 0.7,\ \Lambda = 1.0,\ \beta_1 = 1.0,\ \alpha_T = 10.0,\ \phi = 10.0$. (a) Effect of Darcy number variation, $Re = 1.0$, (b) effect of Reynolds number variation, $Da = 10^{-3}$.

$$\Theta_{\text{int4}} = [0.5576 + 0.4869\varepsilon - 0.0181\Lambda + 60.4243Da - 0.0349Re - 0.0045598\beta_1 - 0.0011282\alpha_T]\Theta_{\text{int1}}. \quad (17)$$

Also, average Nusselt numbers for models II, III and IV in terms of the pertinent parameters and the average Nusselt number for the first model are given below:

$$\overline{Nu_2} = \left[1.0 - 0.0487Da + (12.586\varepsilon + 0.27205\Lambda + 6.8477Re - 5.0257\phi)10^{-6}\right]\overline{Nu_1}, \quad (18)$$

$$\overline{Nu_3} = \left[0.9999 + 0.1952Da + (60.873\varepsilon - 10.0992\Lambda - 14.895Re - 0.91682\alpha_T)10^{-6}\right]\overline{Nu_1}, \quad (19)$$

$$\overline{Nu_4} = [1.5686\varepsilon + 0.0069482\Lambda + 6.0586Da + 0.003314Re - 0.0065775\beta_1 - 0.0015485\alpha_T]\overline{Nu_1}. \quad (20)$$

In the above correlations, Θ_{int1}, Θ_{int2}, Θ_{int3} and Θ_{int4} are the non-dimensional interface temperatures and $\overline{Nu_1}, \overline{Nu_2}, \overline{Nu_3}$ and $\overline{Nu_4}$ are the average Nusselt numbers for models I, II, III and IV, respectively.

4. Conclusions

A comprehensive comparative analysis of the hydrodynamic and thermal interfacial conditions between

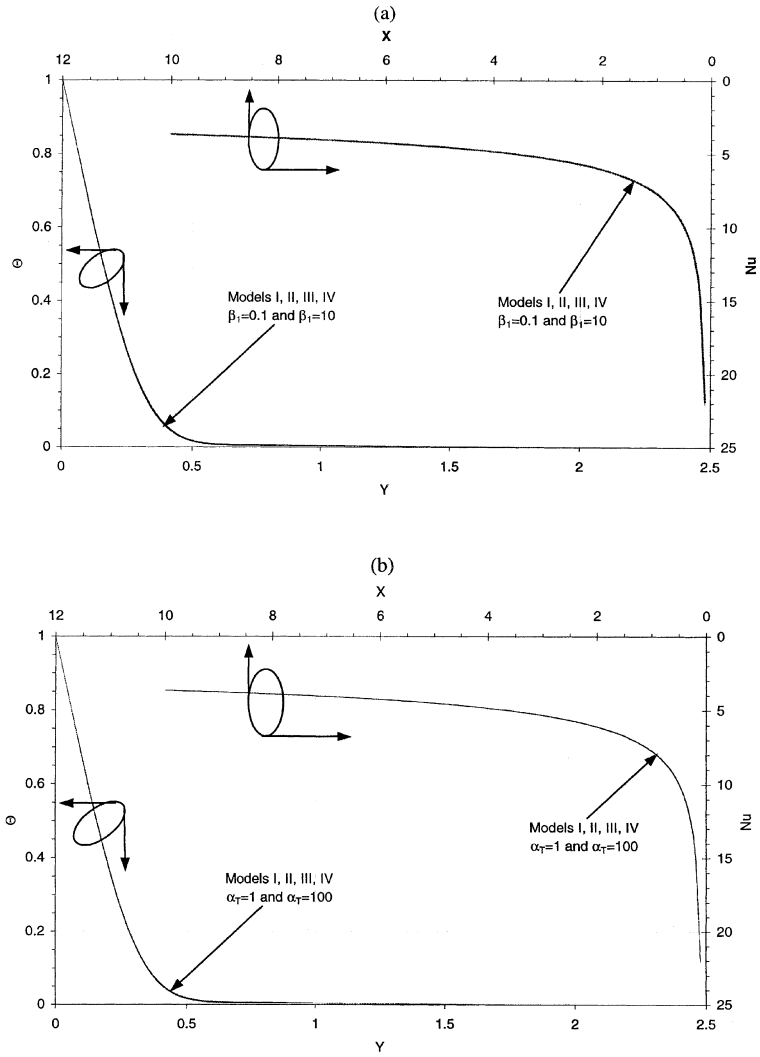

Fig. 12. On the temperature field and Nusselt number distribution for the interface between a porous medium and a fluid layer, $\varepsilon = 0.7,\ \Lambda = 1.0,\ Da = 10^{-3},\ Re = 1.0,\ \phi = 10.0$. (a) Effect of β_1 variation, $\alpha_T = 10.0$, (b) effect of α_T variation, $\beta_1 = 1.0$.

a porous medium and a fluid layer is presented in this work. Five primary categories for the hydrodynamic interface conditions and four primary forms for the thermal interface conditions were analyzed in detail. The main objective of the present study was to analyze the variances among these models and to attest the effects of using them on the characteristics of heat and fluid flow at the interface region. The results of this investigation systematically quantify and characterize the effect of the pertinent controlling parameters on the variances among different interface conditions. It is shown that for most cases the variances within different models, for most practical applications, have a negligible effect on the results while for few cases the variations can become significant. In general, the variances have a more pronounced effect on the velocity field and a substantially smaller effect on the temperature field and yet even smaller effect on the Nusselt number distribution. For hydrodynamic categories, results from models 1 and 5 of Table 1 generate very close results which tend to cluster quite closely and models 3 and 4 generate results which are relatively close to each other, while model 2 generally falls in between these two sets. For heat transfer interface conditions displayed in Table 2, all four categories generate results which are quite close to each other for most practical applications. However, small discrepancies could appear for applications dealing with small values of *Re* and/or larger values of *Da*. The effect of choosing the effective viscosity was found to have a relatively small influence on the velocity field and an

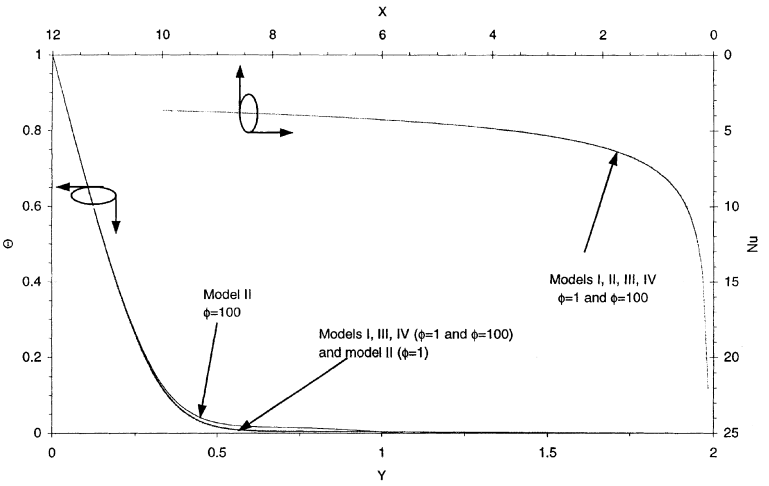

Fig. 13. Effect of ϕ variation on the temperature field and Nusselt number distribution for the interface between a porous medium and a fluid layer, $\varepsilon = 0.7,\ \Lambda = 1.0,\ Da = 10^{-3},\ Re = 1.0,\ \beta_1 = 1.0,\ \alpha_T = 10.0$. (a) $\phi = 1.0$, (b) $\phi = 100.0$.

insignificant effect on the temperature and local Nusselt number distributions. Finally, a set of correlations were provided for interchanging the interfacial velocity, the interfacial temperature and the average Nusselt number among different models.

References

[1] G. Beavers, D.D. Joseph, Boundary conditions at a naturally permeable wall, J. Fluid Mech. 30 (1967) 197–207.

[2] G. Neale, W. Nader, Practical significance of Brinkman's extension of Darcy's law: coupled parallel flows within a channel and a bounding porous medium, Can. J. Chem. Engrg. 52 (1974) 475–478.

[3] K. Vafai, S.J. Kim, Fluid mechanics of the interface region between a porous medium and a fluid layer – an exact solution, Int. J. Heat Fluid Flow 11 (1990) 254–256.

[4] K. Vafai, R. Thiyagaraja, Analysis of flow and heat transfer at the interface region of a porous medium, Int. J. Heat Mass Transfer 30 (1987) 1391–1405.

[5] K. Vafai, S.J. Kim, Analysis of surface enhancement by a porous substrate, J. Heat Transfer 112 (1990) 700–706.

[6] S.J. Kim, C.Y. Choi, Convection heat transfer in porous and overlying layers heated from below, Int. J. Heat Mass Transfer 39 (1996) 319–329.

[7] D. Poulikakos, M. Kazmierczak, Forced convection in a duct partially filled with a porous material, J. Heat Transfer 109 (1987) 653–662.

[8] J.A. Ochoa-Tapia, S. Whitaker, Heat transfer at the boundary between a porous medium and a homogeneous fluid, Int. J. Heat Mass Transfer 40 (1997) 2691–2707.

[9] J.A. Ochoa-Tapia, S. Whitaker, Momentum transfer at the boundary between a porous medium and a homogeneous fluid I: theoretical development, Int. J. Heat Mass Transfer 38 (1995) 2635–2646.

[10] J.A. Ochoa-Tapia, S. Whitaker, Momentum transfer at the boundary between a porous medium and a homogeneous fluid II: comparison with experiment, Int. J. Heat Mass Transfer 38 (1995) 2647–2655.

[11] A.V. Kuznetsov, Influence of the stress jump condition at the porous-medium/clear-fluid interface on a flow at a porous wall, Int. Commun. Heat Mass Transfer 24 (1997) 401–410.

[12] A.V. Kuznetsov, Analytical investigation of the fluid flow in the interface region between a porous medium and a clear fluid in channels partially filled with a porous medium, Appl. Scientific Res. 56 (1996) 53–67.

[13] A.V. Kuznetsov, Analytical investigation of Coette flow in a composite channel partially filled with a porous medium and partially filled with a clear fluid, Int. J. Heat Mass Transfer 41 (1998) 2556–2560.

[14] A.V. Kuznetsov, Analytical study of fluid flow and heat transfer during forced convection in a composite channel partly filled with a Brinkman–Forchheimer porous medium, Flow, Turbulence Combust. 60 (1998) 173–192.

[15] A.V. Kuznetsov, Fluid mechanics and heat transfer in the interface region between a porous medium and a fluid layer: a Boundary Layer Solution, J. Porous Media 2 (3) (1999) 309–321.

[16] J.A. Ochoa-Tapia, S. Whitaker, Momentum jump condition at the boundary between a porous medium and a homogeneous fluid: inertial effects, J. Porous Media 1 (1998) 201–217.

[17] J.A. Ochoa-Tapia, S. Whitaker, Heat transfer at the boundary between a porous medium and a homogeneous fluid: the one-equation model, J. Porous Media 1 (1998) 31–46.

[18] M. Sahraoui, M. Kaviany, Slip and no-slip temperature boundary conditions at the interface of porous, plain media: convection, Int. J. Heat Mass Transfer 37 (1994) 1029–1044.

[19] B. Alazmi, K. Vafai, Analysis of variants within the porous media transport models, J. Heat Transfer 122 (2000) 303–326.

[20] K. Vafai, C.L. Tien, Boundary and inertia effects on flow and heat transfer in porous media, Int. J. Heat Mass Transfer 24 (1981) 195–203.
[21] M. Sahraoui, M. Kaviany, Slip and no-slip velocity boundary conditions at the interface of porous, plain media, Int. J. Heat Mass Transfer 35 (1992) 927–943.
[22] R.C. Gilver, S.A. Altobelli, A determination of the effective viscosity for the Brinkman–Forchheimer flow model, J. Fluid Mech. 258 (1994) 355–370.
[23] J.Y. Jang, J.L. Chen, Forced convection in a parallel plate channel partially filled with a high porosity medium, Int. Commun. Heat Mass Transfer 19 (1992) 263–273.